JOURNAL OF MATERIALS SCIENCE 12 (1977) 1190–1202

The kinetics and mechanism of crystallization in enstatite-type glass-ceramic materials

I. GUTZOW, E. ZLATEVA, S. ALYAKOV, T. KOVATSCHEVA
Institute of Physical Chemistry, Bulgarian Academy of Sciences and Petrurgical Research and Production Corporation, Sofia, Bulgaria

The general crystallization behaviour of a model glass-forming melt having a composition (wt%) 7.5 SiO_2 · 1.0 Al_2O_3 · 1.0 MgO · 1.5 CaO + 10 TiO_2 is investigated. The composition and the morphology of the crystalline phases formed in the system and the structure of the resulting glass-ceramic material are examined by X-ray diffraction, electron microscopy and DTA. Detailed kinetic measurements indicate that the process of nucleation of the initially formed anosovite-type phase may be described from the viewpoint of the non-steady state theory of nucleation. It is also demonstrated that the crystal growth of the spherulites in this phase is diffusion-limited. The role played by TiO_2 in the system under investigation and in similar glass-forming melts is also discussed.

1. Introduction

It was shown recently [1–3] that induced crystallization of glass-forming systems may be quantitatively described as a process of non-steady-state heterogeneous nucleation. A review of the main theoretical and experimental results obtained in these investigations is given in [4].

The problem of the transient character of the nucleation process was raised for the first time by Zeldovich [5] and Frenkel [6]. It can be shown that in principle any phase formation is accompanied by non-steady-state effects [7, 8]. However, in typical glass-forming systems, characterized by a high viscosity, the non-steady-state nature of nucleation may be easily demonstrated [2, 4, 8].

Previous results [1, 2, 4] were obtained on a model single-component phosphate glass $(NaPO_3)_x$; soon afterwards non-steady-state effects were also proved in the crystallization of more complex, two- and three-component silicate systems (e.g. Na_2O–BaO–SiO_2 glasses [9], Li_2O–SiO_2 glasses [10] and Na_2O–CaO–SiO_2 glasses [11]). The transient character of the nucleation kinetics in glass-forming melts was investigated with great accuracy in a recent publication on crystallization in the Li_2O–SiO_2 system [12]. Certain isolated experimental data [13, 14] indicate that possibly non-steady-state effects could be observed also in the crystallization of some glasses in the systems MgO–CaO–Al_2O_3–SiO_2 (+Fe_2O_3) and MgO–Al_2O_3–SiO_2 (+TiO_2).

The analysis of the nucleation kinetics in such silicate systems is of particular interest because the latter constitute the basis of technically interesting glass-ceramic materials. Depending upon the composition of the main crystalline phase which is obtained as a result of the controlled crystallization process (either enstatite $MgSiO_3$ or cordierite $Mg_2Al_3(AlSi_5O_{18})$ the vitrocerams in the system MgO–Al_2O_3–SiO_2 may be placed into the groups enstatite or cordierite. Titania is generally used as nucleator of the crystallization processes in this system. A review of the crystallization processes occurring in enstatite-type glass-ceramics, or the compositions used, of the crystallizations conditions, etc., is given in [15–17].

The present work is mainly concerned with the problem of the applicability of the theoretical concepts of the non-steady-state phase formation used by Gutzow and co-workers [2, 4] to the quantitative description of the nucleation kinetics in typical glass-ceramic materials used in modern technology. The results obtained in

[13–17] encouraged us to study the kinetics of the crystallization process of a model enstatite-type composition in the system MgO–CaO–Al_2O_3–SiO_2 (+TiO_2). The high spherulite density normally reached in the crystallization of technical glass-ceramics greatly hampers the quantitative study of the crystallization process. In order to surmount this difficulty the nucleation and crystal growth kinetics were examined in the present study on thin films blown from the initial glass. The results obtained for the films were then compared with data obtained on massive samples.

The complex composition of the model system and the complicated character of the crystallization processes occurring in it, made it necessary to perform not only purely kinetic measurements but also a number of additional examinations, in order to elucidate the composition and the morphology of the crystalline phases formed. These studies included X-ray diffraction, DTA and electron microscopy.

Particular stress was laid on the effect exerted by liquid–liquid immiscibility occurring in the melt during formation of the glass-ceramics. In fact, liquid-phase separation processes may also proceed under non-steady-state conditions [4, 18]. The transient character of the binodal liquid-phase separation processes was experimentally proved [19] before the non-steady-state character of the crystallization processes in glass-forming systems had been established.

2. Experimental

The main investigations were performed on a glass having a stoichiometric composition 7.5 SiO_2 · 1.0 Al_2O_3 · 1.0 MgO · 1.5 CaO. 10 wt% TiO_2 was added to the initial glass batch.

The glass was cast in steel forms to give 50 mm × 50 mm × 2.5 mm samples which were cooled to room temperature and then annealed at 680° C for 3 h. The annealed glass was transparent, and had no detectable traces of crystallization. The coefficient of thermal expansion, determined by means of a quartz dilatometer, was $\alpha = 50 \times 10^{-7}\ °C^{-1}$.

The temperature dependence of the viscosity, η, up to 810° C and above 1200° C was measured using a platinum rotational viscosimeter for values of log η between 2 and 5, and using a dilatometric viscosimeter for log η ranging between 10 and 13 (Fig. 1). Between 810 and 1200° C the samples crystallized and no η measurements were possible. The transformation range of our glass was determined from the curve as the temperature interval between the annealing point $T_g = 746°$ C (log η = 13) and the softening point $T_f = 796°$ C (log η = 11). The temperature dependence of viscosity for the glass-forming melt under investigation is satisfactorily described by the Vogel–Fulcher–Tammann equation

$$\log \eta = A + \frac{B}{T - T_0} \qquad (1)$$

where in our case $A = -1.22$, $B = 3.6 \times 10^3$ and $T_0 = 500°$ C.

Preliminary crystallization determinations were carried out on a microscope heating stage between 100 and 1400° C.

The two kinds of samples (thin films or glass pieces) were placed on the orifices of a small mobile platinum bridge, to which a Pt–Rh/Pt thermocouple was attached. The bridge was introduced into an electric furnace, maintained at temperatures ranging from 700 to 1000° C (within ±1.5° C); the time of thermal treatment varied from 10 to 600 min.

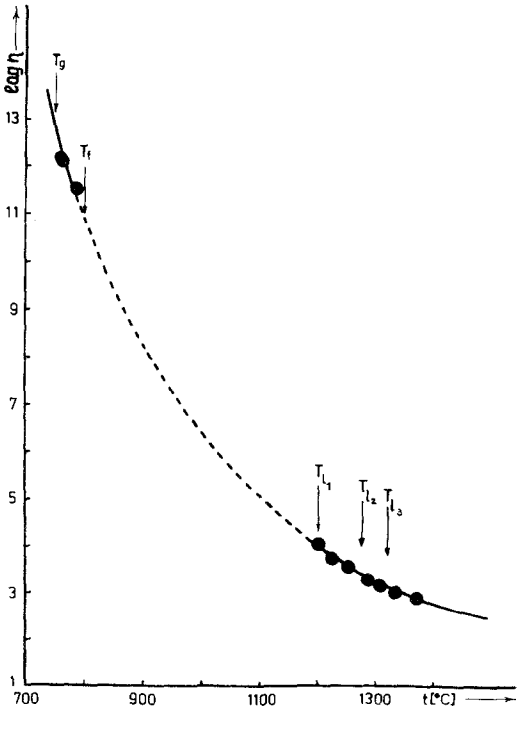

Figure 1 Temperature dependence of the viscosity η of the investigated glass-forming melt. The points T_l denote the melting points of the crystalline phases in the system, according to the DTA results.

Observations on the effect of thermal treatment time showed that the desired temperature in the crystallization furnace is reached after 4 min for the massive samples and after less than 1 min for the thin films. After quenching to room temperature, the samples were examined in polarized transmitted light by means of a Zeiss microscope. Thin sections were prepared from the massive samples, but the glassy films were examined directly. The size of the spherulites was measured using a screw micrometer and their number was determined using a grid micrometer.

The crystallization sequence of the individual phases was determined by DTA. Powdered samples of the initial glass were studied by means of a Linseis DTA instrument within the range 25 to 1500° C, using powdered $\alpha - Al_2O_3$ as standard. The crystalline phases were identified using a Philips X-ray diffractometer (Cu$K\alpha$ radiation).

The microstructure of the massive samples was examined by scanning electron microscopy (JEOL-100B instrument fitted with an SEM attachment). Two-stage replicas (intermediate PVA layer and Pt–C replica) were used as well as samples covered with gold (for SEM examinations). Prior to replication or to gold-shading, the samples were treated with dilute solutions of HF acid.

3. Results of the structural and morphological studies

Fig. 2 illustrates the DTA curve of the composition investigated (heating rate 10° C min^{-1}). The curve is reconstructed from the original recordings after graphical correction for temperature differences between the heated samples and the standard.

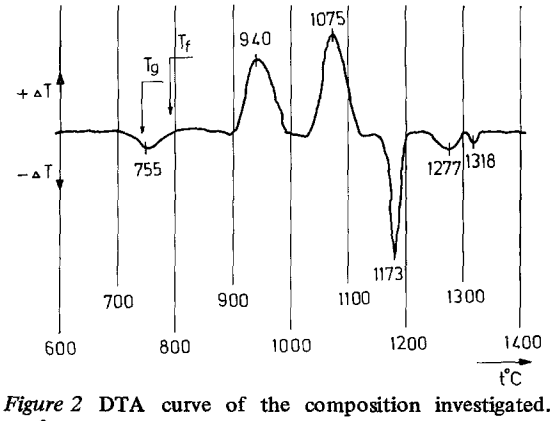

Figure 2 DTA curve of the composition investigated. 755° C – endothermic peak corresponding to transformation range of the glass (T_g and T_f obtained from viscosity measurements); 940 and 1075° C – exothermic crystallization peaks; 1173, 1277 and 1318° C – melting of crystallized phases.

The X-ray studies of the starting glass indicated a complete absence of crystalline phases (Fig. 3, curve 1). Within the 850 to 1200° C temperature interval which, according to [15], is the normal temperature range for the crystallization of an enstatite-type glass-ceramic, the formation sequence of the phases is as follows: between 850 and 950° C a phase forms which is conditionally referred to as anosovite (Fig. 3, curve 2). Upon more prolonged treatment, at the same temperaturee, rutile as well as anosovite is formed as a second phase (Fig. 3, curve 3). Enstatite and α-cristobalite appear as the last phases of the overall crystallization process.

Fig. 3, curve 4 illustrates an X-ray diffraction curve of the model glass-ceramics after a two-stage thermal treatment under conditions similar to those described by Leger and Bray [15]. Diffraction peaks of anosovite, rutile, enstatite and α-cristobalite may be identified.

Comparison of the X-ray diffraction measurements with the DTA results allows the conclusion that the first exothermic peak (at 940° C) in Fig. 2 should probably be attributed to the formation of anosovite and rutile. The second exothermic peak (1075° C) is probably due to the crystallization of enstatite and α-cristobalite. The endothermic peaks should be correlated with the melting of the appropriate crystalline phases.

It has been stressed [15, 17] that only rutile forms upon thermal treatment above 1000° C in samples with a composition similar to that investigated in the present paper. In fact, after heating at 1020° C for 2 h, rutile is the only phase which crystallizes in the samples (Fig. 3, curve 5).

Comparison of the X-ray diffraction experiments with the electron microscope examinations has enabled elucidation of the morphology of the crystalline phases in the present model glass (Figs. 4 to 7). It is seen that in the material investigated, the anosovite phase forms a characteristic spherulitic structure, that rutile appears as thin almost needle-shaped crystals and that enstatite (or α-cristobalite) is formed as isometric, rounded crystals. The very good mechanical properties of the enstatite-type vitrocerams reported in the literature are possibly due to the mutual interpenetration of these different structural components of the material.

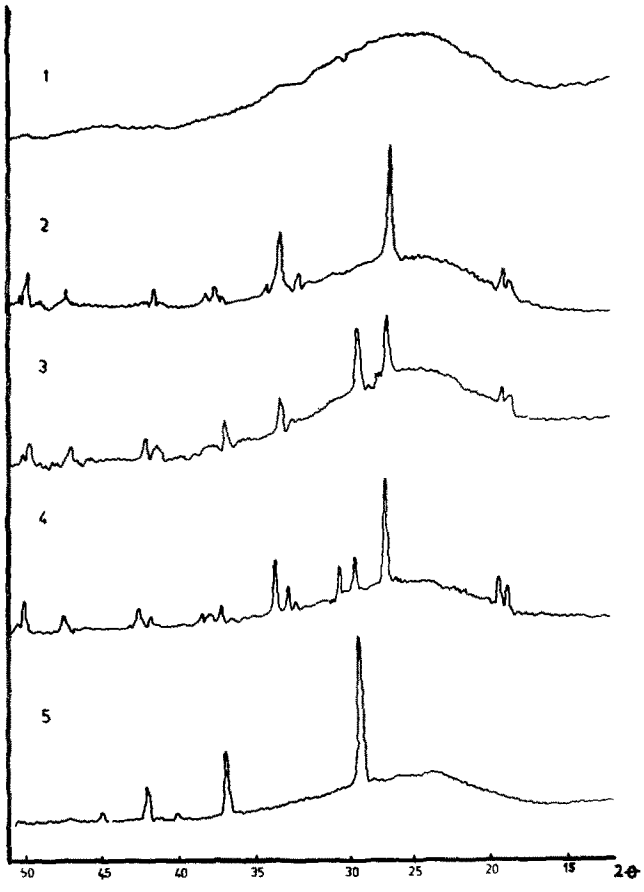

Figure 3 X-ray diffraction pattern of the initial glass and of the crystalline samples: (1) initial uncrystallized glass; (2) sample treated at 907° C for 180 min. Formation of anosovite-type titanates $(Al_2O_3, MgO)\cdot xTiO_2$, (3) sample treated at 907° C for 240 min. Crystallization of anosovite and rutile; (4) sample after two-stage thermal treatment. Crystallization of anosovite, rutile, enstatite, and α-crystobalite; (5) sample containing only rutile after heating at 1020° C for 2 h.

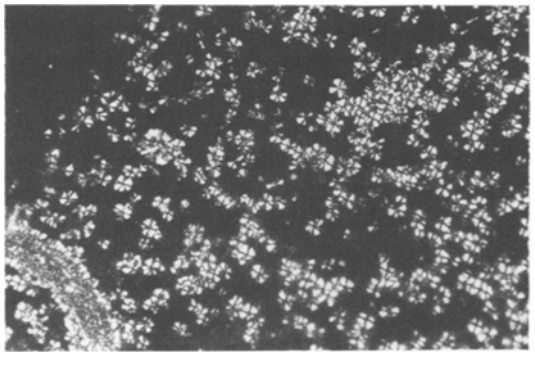

Figure 4 Micrograph of anosovite-type spherulites formed in a thin film sample treated at 907° C for 180 min. Crossed nicols, X 175.

The exact composition of the initially formed anosovite-type crystalline phases is subject to discussion. In the literature [20–22] the formula of anosovite is given as $TiTi_2O_5$ (alternatively as $TiO\cdot 2TiO_2$). The phase $MgO–2TiO_2$ yields an X-ray diffraction pattern nearly identical with that of anosovite [20, 21, 23]. The formation of $TiO\cdot 2TiO_2$ can only occur under reducing conditions [16, 17, 20]. It can therefore be assumed that the first crystalline anosovite-type phase formed with the principal diffraction lines 3.46, 2.84 and 2.18 Å is a magnesium titanate with possibly a high content of the phase $Al_2O_3\cdot TiO_2$ with which it is isomorphous [23]. It proved impossible to determine from the X-ray diffraction patterns whether pure $MgO\cdot 2TiO_2$ formed in the investigated samples, or a phase with a more complex composition. Therefore this anosovite-type phase will be denoted as $(MgO, Al_2O_3)\cdot xTiO_2$.

In the literature [14–17], liquid-phase separation, possibly taking place with the formation of a TiO_2-rich phase as an initial or even necessary stage in the formation of $MgO–(CaO)–Al_2O_3–SiO_2$ vitrocerams "initiated" with TiO_2, is discussed in detail. Electron microscope examination showed that there was no typical liquation pattern in the initial annealed samples (Fig. 8). When massive samples were treated at about 900° C for 15 min (i.e. under conditions where no crystallization is detectable by X-ray diffraction) a

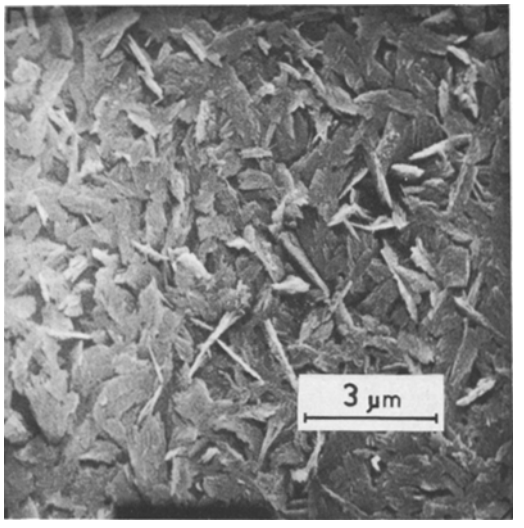

Figure 5 Anosovite-type spherulites in massive samples treated at 907° C for 180 min. SEM of a freshly fractured sample, treated for 1 min with 5% hydrofluoric acid.

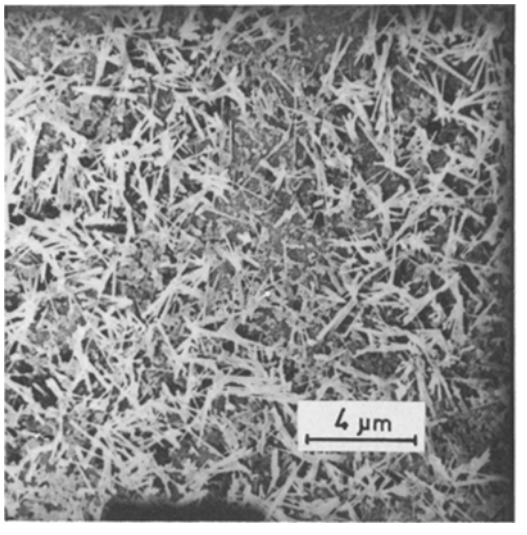

Figure 6 SEM of rutile crystals in a freshly fractured sample, treated for 1 min with 5% hydrofluoric acid (sample from Fig. 3, curve 5).

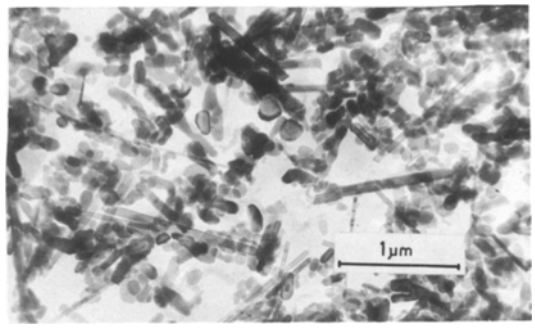

Figure 7 Electron micrograph of a fully crystallized sample. Needle-shaped rutile and isometric enstatite crystals lifted by the Pt–C replica. Fractured sample, treated for 1 min with 5% HF.

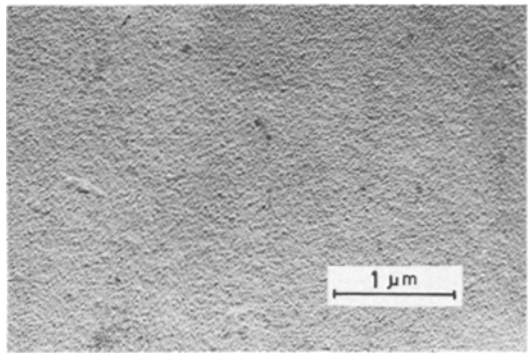

Figure 8 Electron micrograph of a sample of the initial glass surface treated for 10 sec with 2.5% HF, Pt–C replica.

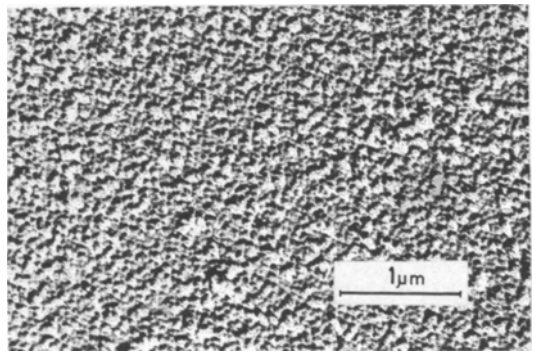

Figure 9 Electron micrograph of a sample heat-treated at 907° C for 15 min. Surface treated with 2.5% HF. Pt–C replica.

pattern was obtained which could be referred to as a process of liquid-phase separation (Fig. 9). However, it was impossible to tell whether this was a typical case of liquid–liquid immiscibility or some form of structural inhomogeneity in the heat-treated glass, developed by the HF-leaching. It is interesting to note that whereas the number of structural elements in Fig. 9 (perhaps liquation domains) is about 2.5×10^{15} cm^{-3}, the number of anosovite spherulites in massive samples (Fig. 5) treated at similar temperatures is about 1.5×10^{11} cm^{-3}. Therefore, a correlation between structural elements in Fig. 9 and the formation of the first crystalline phase (anosovite $(MgO, Al_2O_3)\cdot xTiO_2$) should not be expected.

4. Some basic theoretical considerations

As shown in [4], in order to elucidate the kinetics of nucleation, it is sufficient in most cases to analyse the character of the $N(t)$–t curves (number N of nuclei grown at time t). When transient effects are negligible, the stationary rate of nucleation is instantaneously established. In this case, according to

$$N(t) = \int_0^t I(t) \cdot \mathrm{d}t \qquad (2)$$

with a constant nucleation rate $I(t)$, i.e.

$$I(t) = \text{const.} = I_0$$

a linear dependence between the number of nuclei N and the time t is followed:

$$N(t) = I_0 t. \qquad (3)$$

Under non-steady-state conditions as a first approximation* [4, 5, 8],

$$I(t) = I_0 \exp.\left(-\frac{\tau}{t}\right) \qquad (4)$$

is obtained, where τ is the transient time lag. Using Equations 2 and 4, the following expression can be derived†:

$$N(t) = I_0 t\left[\exp\left(-\frac{\tau}{t}\right) + \frac{\tau}{t}\,\mathrm{Ei}\left(-\frac{\tau}{t}\right)\right] \qquad (5)$$

which may be approximated by an $N(t)$–t curve shifted with respect to the origin, by $b\tau$ (Fig. 10a), where $b \approx \pi^2/6$.

Strictly speaking, Equations 3 and 5 refer only to the case of homogeneous nucleation. In the case of heterogeneous nucleation, when M highly active crystallization sites are present per unit volume of the melt (e.g. insoluble crystallization cores) the nucleation process will proceed in practice only over them. In such a case under stationary conditions, the heterogeneous nucleation rate I_0^* will be time-dependent owing to the depletion of the initial active sites. Then, using Equation 2, it follows that

$$N(t) = M[1 - \exp(-I_0^* t)]. \qquad (6)$$

In the case of heterogeneous non-steady-state nucleation on M active sites as shown in [4]

$$N(t) = M\left[1 - \exp\left\{-I_0 t\left[\exp\left(-\frac{\tau}{t}\right) + \frac{\tau}{t}\,\mathrm{Ei}\left(-\frac{\tau}{t}\right)\right]\right\}\right]. \qquad (6a)$$

These two dependences are illustrated in Fig. 10b. It is seen once again that the curve for the transient case is shifted with respect to the origin by $b\tau$. This shift, as in the homogeneous case, is the fundamental experimental criterion for determining the character of the nucleation process (stationary or non-steady-state). It should be borne in mind, however, that curves similar to those given in Fig. 10b are to be expected, in principle, for the advanced stages in the case of homogeneous nucleation since every process of phase formation is accompanied by a depletion of the space available for nucleation (either by the growing crystallites themselves or by diffusion zones [24]. Consequently, strictly speaking, the curves in Fig. 10a should be considered only as an approximation of the initial stages of nucleation.

Taking into account results given in [4] and [8], it is possible to represent the temperature dependence of I_0 with sufficient accuracy as

$$I_0 \simeq \text{const.}\,\frac{1}{\eta}\exp\left(-\frac{K_3}{T\Delta T^2}\right) \qquad (7)$$

i.e. the steady-state nucleation rate is determined by the temperature dependence of the viscosity η of the crystallizing melt and by the undercooling $\Delta T = T_m - T$. At sufficiently small temperature intervals, the temperature dependence of viscosity

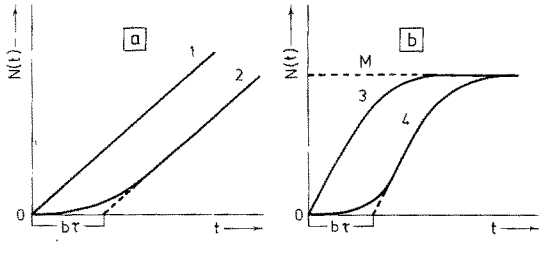

Figure 10 Theoretical $N(t)$–t curves. (a) Homogeneous nucleation (initial stage): curve 1, stationary process; curve 2, non-steady-state nucleation. (b) Heterogeneous nucleation: curve 3, stationary case; curve 4, non-steady-state case.

* For a more precise solution see [7, 8].

† Here Ei denotes the integral exponent function.

may be represented by an exponential expression instead of the Vogel–Fulcher–Tamman equation:

$$\eta = A \exp\left(\frac{U_\eta}{RT}\right), \qquad (8)$$

where U_η denotes the activation energy of viscous flow in the temperature interval under consideration. For crystallization of multi-component melts, the melting temperature, T_m, should be replaced by the corresponding liquidus temperature, T_l, i.e. $\Delta T = T_l - T$.

In the presence of M strongly active crystallization cores, the maximum number, N_s, of crystallites in the saturated region of the $N(t)$–t curves will be directly equal to M [4, 24]. If all introduced crystallization cores have equal activities, Φ, with respect to the crystallization process, then N_s, irrespective of the conditions (temperature, supersaturation) will be constant. In some cases it is possible that the activity Φ with respect to the crystallization process is different (for instance, due to the different degree of disorder in the structure, to the different size of the individual cores, etc.). In this case the saturated number of crystallites N_s for different temperatures will be different since, according to the basic formula of heterogeneous nucleation,

$$I_0 = \text{const.}\frac{1}{\eta} \cdot \exp\left(-\frac{K_3\Phi}{T \cdot \Delta T^2}\right)$$

and Equations 6 and 6a, the number, N of crystallization cores developed at a given temperature will be a function of the nuclei activity Φ_i. The case of heterogeneous nucleation on differently active nuclei is discussed (applied to electrocrystallization) in [25].

In the homogeneous case, the number of crystallites formed in the melt under given conditions, i.e. the final dispersity of the new phase, is generally a function of the ratio I/V, where V is the growth rate of the individual spherulites [26]. More precisely, by applying the formula of the Kolmogrov–Avrami equation, the maximum number, N_s, of the crystallites formed in a melt according to Erofeyev [27] will be

$$N_s = \frac{I_0^{3/(q+3)}}{V^{q/(q+3)}} \qquad (9)$$

where q is a factor depending on the type of the crystallization process.

Markov and Kashchiev's exhaustive study [24] indicates that also in the presence of active cores, conditions exist under which (at small values of I_0^* or large values of V) N_s will not be directly determined by M, but will be a function of the same type as Equation 9.

The temperature dependence of the time lag τ according to [4] and [7] is given by

$$\tau = a \cdot \sigma \cdot \left(\frac{N_A}{\lambda_m}\right)^2 \cdot \left(\frac{T_m}{\Delta T}\right)^2 \cdot d_0^5 \cdot \eta \cdot \frac{1}{Z'} \qquad (10)$$

where the constant $a \approx 1$, N_A is Avogadro's number, d_0 is the mean interatomic distance in the melt, σ is the surface energy of the interface initial phase–newly formed phase, and λ_m is the corresponding heat of transition. The factor Z' in Equation 10 takes into account the difficulties inherent to the incorporation of the molecules of the initial phase in the critical nucleus of the new phase. When the latter is isotropic (for example, in the case of liquid phase separation) [8, 18] $Z \approx 1$, whereas upon formation of crystalline phases the condition for the retention of the equilibrium form of the nucleus, when the possible growth sites on its faces are taken into account, leads to an estimate of $Z' \approx 10^{-3}$ to 10^{-6} [4, 8].

In most technically interesting systems, the values of the constants involved in Equation 10 are unknown. In order to estimate the expected values of the surface energy, σ, at the crystal melt interface, the Turnbull–Scapski equation [28] can be used:

$$\sigma = \gamma_0 \cdot \frac{\lambda_m}{N_A^{1/3} \cdot \tilde{V}_m^{2/3}}, \quad \gamma_0 \approx 0.5,$$

where $\tilde{V}_m$ is the volume of a molecule in the crystal.

In addition, the heat of melting may be represented as $\lambda_m = \gamma_1 R T_m$ where, for simple melts, γ_1 is of the order of 1.0 to 1.5. Thus, it follows from Equation 10 (with $\tilde{V}_m \approx d_0^3$)

$$\tau \cong a \frac{\gamma_0}{\gamma_1} \cdot \frac{1}{kT_m} \cdot \frac{d_0^3}{Z'} \cdot \eta \left(\frac{T_m}{\Delta T}\right)^2. \qquad (11)$$

If T/T_m (or T/T_l for multicomponent systems) is denoted by x and the values of the constants involved in Equation 11 are introduced, we obtain for substance having T_m (or T_l) $\approx$

1000 to 1500° C as is the case for most silicate materials

$$\tau \cong 10^{-8} \cdot \frac{\eta}{Z'} \cdot \left(\frac{1}{1-x}\right)^2 . \qquad (12)$$

It follows that measurable non-steady state effects ($\tau \geqslant 10^3$ sec) should be expected when at $x = 0.8$ to 0.7, viscosity of the order 10^6 to 10^8 P is reached.

The time required for reaching a given degree of crystallization, e.g. the time τ_1 for the formation of the first nucleus, is often determined experimentally. If no transient effects are involved $\tau_1 = 1/I_0$. In the non-stationary case the dependence between τ_1 and I_0 may be represented approximately as [4]

$$\tau_1 \cong \frac{1}{I_0} + b\tau .$$

It is evident that when $b\tau \gg 1/I_0$, the time required for the appearance of the first nucleus (or the time necessary to produce the first trace of crystalline opalescence in the melt) will be directly determined by τ rather than by I_0.

The non-steady-state effects may also determine the considerable induction periods in the curves relating the mean size, l, with time which describe the growth of spherulites in the melt. On the other hand, the analysis of spherulite growth makes it possible to estimate the time required for the critical nucleus to grow from Gibbs–Thomson to visible size. This is necessary, as will be shown later, in order to decide whether the experimentally observed induction periods in l–t curves are not determined by the time needed for growth up to visible size. As indicated by Gutzow and co-workers [1, 2], such growth effects could also lead to a shift of the $N(t)$–t curves.

As upon crystallization of glass-forming systems growth proceeds so sluggisly that the self-heating of the growing spherulite is precluded, a time–linear growth process should be expected in the case of crystallization of simple melts, $l = Kt$, i.e.

$$V = \frac{dl}{dt} = K . \qquad (13)$$

In the case of crystallization of one component in a multicomponent melt, it will be a diffusion-limited growth

$$l = Kt^{1/2} , \qquad (14)$$

i.e.

$$V = \frac{dl}{dt} = \frac{K}{2} \cdot t^{-1/2} . \qquad (15)$$

In the presence of an induction period the above dependences become respectively

$$l = K(t-\tau) \qquad (13a)$$

$$l = K(t-\tau)^{1/2} . \qquad (14a)$$

For spherulite sizes l, commensurable with the size l^* of the critical nucleus the growth rate for the two cases (Equations 13 and 15) should be multiplied by $(1 - l^*/l)$ which takes into account the Gibbs–Thomson effects [29].

As shown by Markov and Kashchiev [24] in the case of diffusion-limited growth, the saturated number of crystallites will be given, as in the case of Equation [9], by the expression

$$N_s = \text{const.} f(2q+1) \cdot \frac{I^{2q+1}}{K} , \qquad (16)$$

which, obviously, will also hold in those cases of heterogeneous nucleation in which the growth rate of the crystallites, or of the diffusion zones around them, is higher than the rate of nucleation. With sufficiently active nuclei, $N_s \approx M$ once again.

5. Experimental data and discussion of the nucleation and crystal growth kinetics

Fig. 11 illustrates the results of a series of measurements giving the number N of $(MgO \cdot Al_2O_3)x TiO_2$ spherulites as a function of time upon thermal treatment of the initial glass at several different temperatures. An induction period is visible, followed by a linear increase of the number of spherulites and a saturation region. It is also seen, in spite of the rather scattered experimental data, that the maximum number of spherulites in the saturation region increases relatively weakly with temperature.

In Fig. 12 the experimental data on the temperature dependence of the viscosity, η (Fig. 1 and Equation 1) for the same temperature interval, is given according to Equation 8 as log η versus $1/T$. In the same figure, the induction period from Fig. 11 is given as log τ versus $1/T$ according to Equations 8 and 10. It is seen that in the relatively small temperature region under consideration,

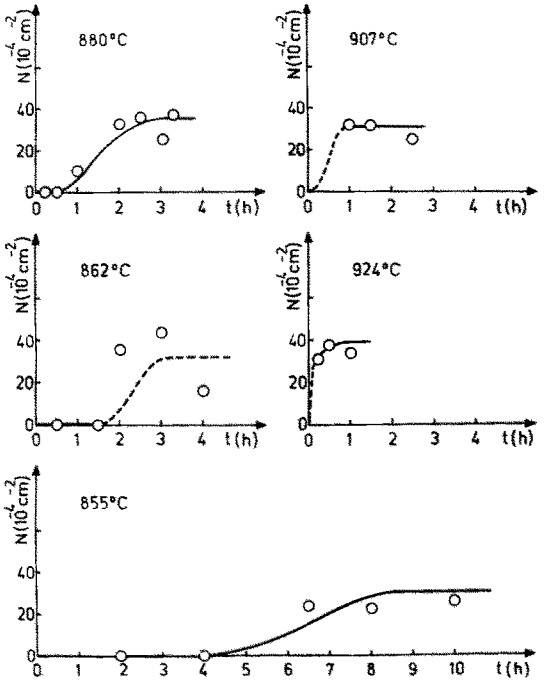

Figure 11 Experimental $N(t)$–t curves for the crystallization of $(Al_2O_3, MgO)\cdot xTiO_2$ for different temperatures. Measured on thin films.

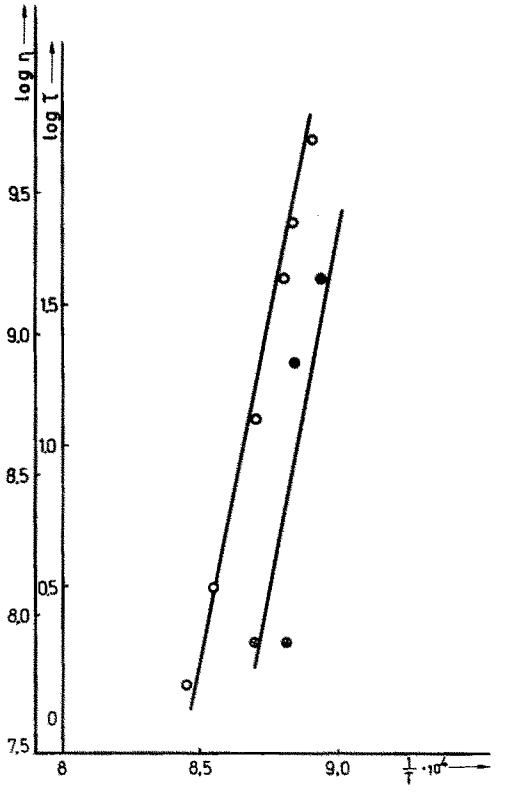

Figure 12 Induction period of nucleation τ as $\log \tau$ versus $1/T\bullet$, and the temperature dependence of η as $\log \eta$ versus $1/T\circ$.

both $\log \eta$ and $\log \tau$ are linear with respect to $1/T$. Moreover, for both quantities, an almost equal value of effective activation energy $U_\eta = U_\tau = 163\,\text{kcal mol}^{-1}$, can be determined.

Data concerning the growth of $(MgO\cdot Al_2O_3)\cdot xTiO_2$ spherulites during the initial period of phase formation are given in Fig. 13. It was found that the induction period, τ, which can be observed in the growth of spherulites (Fig. 13) is almost identical to the induction period of nucleation determined for the $N(t)$–t curves for films. As seen from Fig. 14, these induction periods are in good agreement with the induction periods determined from thin sections of massive samples as the time of the first microscopically visible crystallization.

Fig. 15 shows that according to Equation 14a, the data concerning spherulite growth (Fig. 13) yield straight lines for plots of l versus $\sqrt{(t-\tau)}$, where l is the mean size of the spherulites at time t. According to the discussion in the previous paragraph, the crystal growth in the vitroceram-forming melt investigated may be interpreted as a diffusion-limited growth.

Equation 14a may be written as

$$l = \text{const.}\sqrt{D(t-\tau)}^{1/2}. \qquad (17)$$

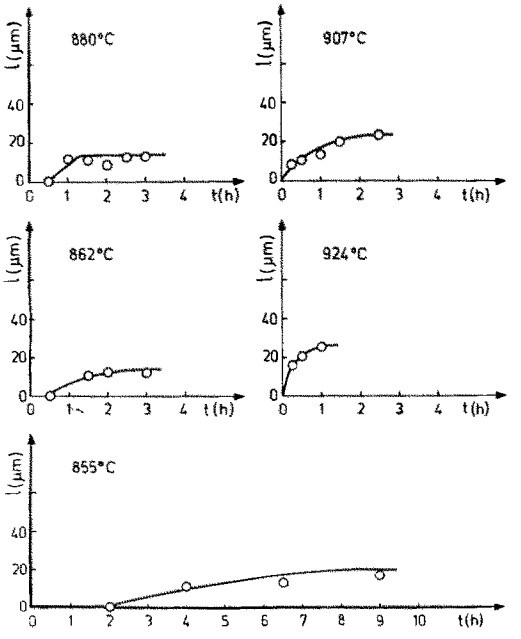

Figure 13 Change in the mean size l of $(Al_2O_3, MgO)\cdot xTiO_2$ spherulites with time at different temperatures as observed on thin films.

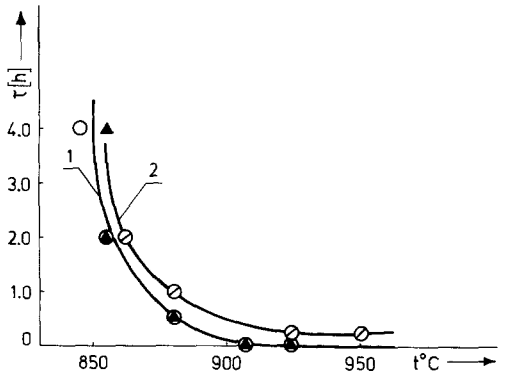

Figure 14 Comparison between the induction period τ measured in thin films and in massive samples. Curve 1 results for thin films: ○, data taken from $N(t)$–t curves; ▲, data taken from l–t cufves. Curve 2: ⦶ induction periods determined in massive samples as the first microscopically detectable crystallization (in crossed nicols).

For the mean diffusion coefficient, $D \simeq K^2$, a temperature dependence of the type

$$D \simeq \text{const.} \exp\left(-\frac{U_D}{RT}\right) \qquad (18)$$

may be most generally expected.

Fig. 16 indicates that, in fact, the temperature dependence of D may be represented by Equation 17. For U_D a value of 109 kcal mol^{-1} is obtained. Therefore, $U_\eta \approx 1.5\ U_D$, i.e. the activation energy of crystal growth in the melt, determined in this way, is considerably lower than the activation energy both of the induction period, τ, and of the viscous flow of the melt.

Figs. 11 and 13 show that the induction periods, τ, observed both in growth and nucleation, are of the order of several hours. In principle they include: (1) the time, τ_0, required for the onset of supersaturation in the system, i.e. the time required for the sample to reach a given temperature after its introduction into the furnace; (2) the time required to reach a steady-state distribution of the subcritical nucleation complexes, i.e. the non-steady-state time-lag, τ; and (3) the time required for the formation of the first nucleus, τ_1 (which can be determined from the slope of the $N(t)$–t curves in the linear region as $\tau_1 = 1/I_0$); (4) the time τ_2 required for growth from Gibbs–Thomson size (10^{-6} to 10^{-7} cm) to a size visible, for instance, in an optical microscope ($\sim 10^{-4}$ cm). As in our case $\tau_0 \approx 1$ min, and as $1/I_0$ is also negligible compared with the observed induction periods τ (as seen from Fig. 11), possibilities 2 and 4 must be discussed. It is clear that if $\tau \gg \tau_2$, non-steady-state nucleation will control the whole crystallization process in the system; on the contrary, if $\tau_2 > \tau$ the observed induction periods are to be treated as growth times. The numerical estimates performed to this effect by extrapolating the experimental growth data on the log l versus log $(t-\tau)$ plot to Gibbs–Thomson size, showed that the time τ_2 required for growth from 10^{-6} to 10^{-4} cm is about 4 to 5 min. Therefore, the induction periods observed may be considered as non-steady-state time lags, and the investigated crystallization process should be treated as an example of non-steady-state nucleation.

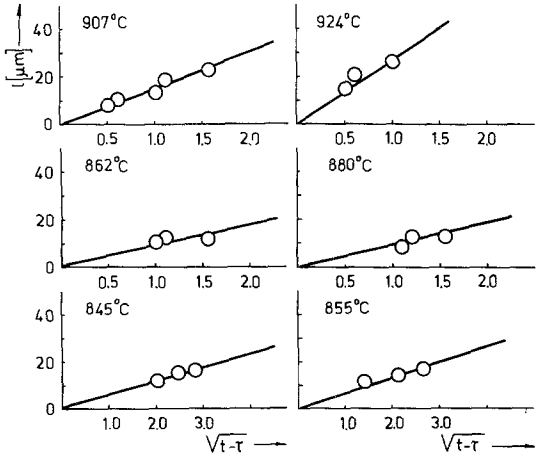

Figure 15 Data from Fig. 13 for the growth of $(Al_2O_3, MgO) \cdot xTiO_2$ samples plotted as l versus $\sqrt{(t-\tau)}$.

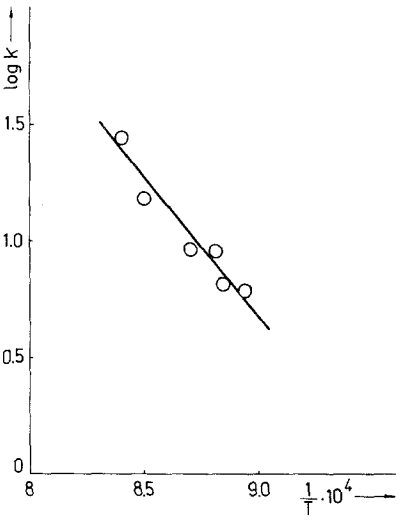

Figure 16 Determination of the temperature dependence of the coefficient K from growth isotherms for anosovite-type spherulites.

The N_s values from Fig. 11 can be considered as increasing with temperature from 30×10^4 (at 855° C) to 40×10^4 cm^2 (at 924° C); this increase is possible within the limits of the experimental error for the measurements analysed.

From the discussion in Section 4, it can be seen that this tendency (if it exists) makes it unnecessary to consider curves of Fig. 11 as a case of heterogeneous nucleation on a constant number M of very active crystallization cores having equal activity. In this case the saturated portion of the $N(t)$ curves in Fig. 11 could be interpreted either as being determined by the exhaustion of the volume accessible to nucleation upon homogeneous nucleation, or as heterogeneous nucleation on relatively inactive crystallization cores. It is also interesting to note that in the linear portions of the $N(t)$–t curves, the ratio I_0/K is an increasing function of temperature, i.e. it is possible that it predicts the temperature dependence of N_s according to Equation 16.

6. General discussion

The present investigation leads to some general conclusions concerning the kinetics of nucleation and the mechanism of crystallization during the formation of glass-ceramics. In estimating the validity of these conclusions, it should be taken into account that:

(1) the complexity of the model did not allow a sufficiently complete and exhaustive study of the kinetics of the crystallization processes as proved possible for simpler one-component model glass-forming systems (for example, $NaPO_3$ [2, 4]);

(2) only the crystallization of the initially formed phase could be studied quantitatively.

According to the arguments in Section 5, the induction periods observed in the $N(t)$–t and in the l–t curves may be treated as a non-steady-state time lag. This also follows from the estimate of τ which can be made using Equation 12 for the following conditions: $T \simeq 1200$ K, $T_m \simeq 1550$ K, i.e. $x \simeq 0.8$ and (from Fig. 1) $\eta = 10^8$ to 10^9 P. With these values of η and x, at $Z' = 1$, $\tau \simeq 10$ sec and at $Z' = 10^{-2}$, $\tau \simeq 10^3$ sec. Conversely, the experimental values of τ and the values of η at the corresponding temperatures, yield from Equation 12 values of $Z' \simeq 10^{-3}$ to 10^{-2}, which are quite reasonable, taking into account that this is the formation of a crystalline phase.

Similar values for Z' were in essence also found by James [12] in the crystallization study of Li_2O–SiO_2 glasses. In the case of crystallization of $NaPO_3$ glasses, even lower values were found for Z' [2, 4].

If the present results are compared in more detail with the data obtained for the model $NaPO_3$ glass [1–4] it can be seen that in the case of $NaPO_3$: (1) the crystallization process which takes place in a one-component system is not diffusion-limited, i.e. the curves are described by Equation 13a and (2) the nucleation process is a typical heterogeneous process in which the number of spherulites corresponds directly to the number of introduced crystallization cores (platinum or other noble metal particles).

Unlike the one-component system cited, the crystallization process of $(MgO, Al_2O_3)\cdot xTiO_2$ which proceeds in a multi-component system (i.e. with a diffusion zone in the residual melt remaining around the growing spherulites) is diffusion-limited and is described by Equation 14a. The presence or absence of a diffusion-hindering effect should not exert a substantial effect on the time lag τ, since around the critical nucleus ($l = l^*$) for which the growth rate is equal to zero ($1 - l^*/l = 0$), there should be no diffusion zone. This means that, in principle, this case could also be described by Equations 10 and 12.

It has already been noted that the activation energy U_D for the growth of $(MgO, Al_2O_3)\cdot xTiO_2$ is lower than the activation energy of viscous flow U_η which determines the induction period τ. Such a ratio between U_η and U_D has been observed [30] for the model glass $(NaPO_3)x$ and, apparently, for certain other glass-forming systems. Possibly this means that for the growth of crystallites already formed the necessary reorganization of structural elements of the melt is less drastic than for viscous flow and formation of nuclei of the new phase.

It is widely accepted that the role of TiO_2 in the crystallization of glass-ceramics reduces to the formation of crystallization cores for heterogeneous nucleation, in most cases via liquid-phase separation. It is believed that the newly formed phase boundaries (TiO_2-rich droplets or rutile) induce the separation of the corresponding crystalline phases.

The present investigation gives no direct evidence that the crystallization of $(Al_2O_3, MgO)\cdot xTiO_2$ is a case of heterogeneous nucleation on really active crystallization cores. This is so because, on the one hand, as indicated in

Section 5, the number of spherulites N_s depends on temperature and, on the other (cf. Section 3), there is no direct correspondence between the number N_s of the $(MgO, Al_2O_3)\cdot xTiO_2$ crystals formed (Fig. 5) and that of the structural inhomogeneities visible in Fig. 9, if the latter are considered as the nucleating cores of the crystallization process.

In making an assessment of the role of TiO_2 in the formation of enstatite-type glass-ceramics, it should be taken into account that TiO_2 participates in the chemical composition of the initial crystalline phases (anosovite and rutile), and it is possible that they also serve as crystallization cores in the crystallization of later phases (enstatite, α-cristobalite). Furthermore, it is important to note that titania generally decreases the melting temperatures of the crystalline phases which are formed in the system under investigation. A more general discussion on the activity of crystallization cores is given in [31].

The results of the present investigation show that non-steady-state effects may be of decisive importance in the interpretation of the crystallization phenomena in glass-ceramic materials, especially when the viscosity of the system is more than 10^7 to 10^9 P. From this viewpoint, for example, it becomes clear that the induction period, usually determined as the time of the first microscopically visible crystallization in the samples at the given viscosities, does not yield crystallization rates (via $I_0 = 1/\tau_1$) but rather a non-steady-state time lag τ (cf. Fig. 14). Taking into account our results, it is also very possible that the relatively large induction periods observed by some other authors in the $N(t)$–t [13, 14] curves of cordierite- or enstatite-type systems, as well as the induction periods in the curves describing the overall crystallization of cordierite-type ceramics observed by Zdaniewski [14] are also determined by non-steady-state effects. In the papers quoted, however, there are no viscosity data, so that even the semi-quantitative estimations given here for the absolute value of τ cannot be performed.

Acknowledgements

We wish to thank Professor R. Kaischew and Dr C. N. Poulieff for helpful discussions of some of the main results of the present investigations. Thanks are also due to Dr M. Marinov and Dr I. Tomov for help in solving some experimental problems.

References

1. I. GUTZOW, E. POPOV, S. TOSCHEV and M. MARINOV, Proceedings of the Symposium on Crystal Growth, VII ICC, Moscow, July 1966, Rost Kristallov, vol. VIII, Part II (Izd. Nauka, Moskwa, 1968) p. 95.
2. I. GUTZOW, S. TOSCHEV, M. MARINOV and E. POPOV, *Kristall u. Technik* **3** (1968) 37, 337, 485.
3. S. TOSCHEV and I. GUTZOW, *Phys. Stat. Sol.* **21** (1967) 683.
4. I. GUTZOW and S. TOSCHEV, in "Advances in Nucleation and Crystallization in Glasses", edited by L. L. Henche and S. W. Freiman (Amer. Ceram. Soc., Columbus, Ohio, 1971) p. 10.
5. J. B. ZELDOVICH, *Acta Physiocochem, URSS* **18** (1943) 1.
6. J. FRENKEL, "Kinetic Theory of Liquids" (Dover, New York, 1955) p. 398.
7. D. KASHCHIEV, *Surface Sci.* **14** (1969) 209.
8. S. TOSCHEV and I. GUTZOW, *Kristall u. Technik* **7** (1972) 43.
9. D. G. BURNETT and R. W. DOUGLAS, *Phys. Chem. Glasses* **12** (1971) 117.
10. V. N. FILIPOVICH and A. M. KALININA, *Neorg. Mat.* **6** (1970) 351.
11. Z. STRNAD and R. W. DOUGLAS, *Phys. Chem. Glasses* **14** (1973) 33.
12. P. F. JAMES, *ibid* **15** (1974) 95.
13. P. R. ROGERS, *Mineralog. Mag.* **37** (1970) 741.
14. W. ZDANIEWSKI, Ph. D. Thesis, University of Gothenburg (1975).
15. L. LEGER and J. BRAY, *Glass Technol.* **7** (1966) 134.
16. L. LEGER and J. BRAY, *Silicates Ind.* **33** (1966) 275.
17. E. PLUMAT, *ibid* **38** (1972) 97.
18. I. GUTZOW, in "The Vitreous State" (Disc. Faraday Soc. No 50, London, 1971) p. 236.
19. J. J. HAMMEL, *J. Phys. Chem.* **46** (1967) 2234; S. M. OHLBERG and J. J. HAMMEL, Proceedings of the VII International Congress on Glass, Brussels, 1965, Number 32, p. 1.
20. D. BELYANKIN and W. LAPIN, *Doklady ANSSSR* **80** (1951) 421.
21. A. WINCHELL and H. WINCHELL, "Optical Properties of Artificial Materials" (Academic Press, New York, London, 1964).
22. J. D. H. DONNAY, "Crystal Data" ACA Monograph No. 3 (Amer. Crystallograph. Assoc., Washington D.C., 1963).
23. T. YOSHIDA, H. UEOKA and T. TAKEI, *J. Electrochem. Soc. Japan (Overseas Suppl. Ed.)* **28** (1960) E 257.
24. I. MARKOV and D. KASHCHIEV, *J. Crystal Growth* **13/14** (1972) 131.
25. R. KAISCHEW and B. MUTAFTSCHIEW, *Electrochem. Acta* **10** (1965) 643.
26. M. VOLMER, "Kinetik d. Phasenbildung" (Verl.Th.Steinkopf, Dresden u. Leipzig, 1939) p. 206.
27. B. V. EROFEYEV, Sbornik nauchnich Tabot, ANBSSR, Inst, Khim. No 5 (1) (Izd. ANBSSR, Minsk, 1956) p. 13.

28. D. TURNBULL and M. H. COHEH in "Modern Aspects of the Vitreous State", edited by I. D. Mackenzie (Butterworths, London, 1960) p. 38.
29. R. J. SCHAEFER and M. E. GLICKSMAN, *J. Crystal Growth* **5** (1969) 44.
30. I. GUTZOW and I. KONSTANTINOV, *Compt Rend.* (Bulgarian Academy of Sciences) **23** (1970) 1107.
31. I. GUTZOW, *Glastech. Ber.* **46** (1973) 221.

Received 25 August and accepted 8 November 1976.